Mott-Schottky Analysis of Nanometer-Scale Thin-Film Anatase TiO_2

R. van de Krol, A. Goossens,* and J. Schoonman*

Laboratory for Applied Inorganic Chemistry, Delft University of Technology, 2628 BL Delft, The Netherlands

ABSTRACT

Smooth nanometer-scale films of anatase TiO_2 on indium-tin oxide substrates (ITO) are obtained by electron-beam evaporation of reduced TiO_2 powder. Mott-Schottky analysis shows an abrupt change in slope when the depletion layer reaches the TiO_2/ITO interface. An electrostatic model is derived, which gives a quantitative description of the observed change in slope. From the potential at which the slope changes, the dielectric constant of anatase could be accurately determined. A value of 55 is found, which is significantly lower than those reported for anatase TiO_2.

Introduction

Recently, much attention has been focused on the use of nanostructured metal oxide semiconductors for various applications, such as electrochromic windows,[1] photocatalytic devices,[2] lithium-ion batteries,[3] dielectrics in integrated circuits,[4] and dye-sensitized TiO_2 solar cells.[5] In porous nanostructured films, the fraction of atoms located at or near the surface is very large. For example, in spherical anatase TiO_2 particles with a diameter of 5 nm, approximately 7% of the atoms is located at the surface, and an even larger fraction of the atoms is in proximity to it and experiences an anisotropic environment. This has a significant effect on the electronic structure, as well as on the related opto-electronic properties of porous nanostructured semiconductors. Due to the large specific surface area, there is an accompanying large number of chemical reaction and/or adsorption sites present. This feature is used in dye-sensitized TiO_2 solar cells, in which the nanoporous structure allows a huge increase in the number of adsorbed dye-molecules (compared to flat surfaces), thereby greatly enhancing the efficiency of the device.[5]

* Electrochemical Society Active Member.

Improving existing devices based on porous nanostructured TiO_2, and developing new ones, requires detailed understanding of the fundamental properties of (nanostructured) anatase TiO_2. Although a vast number of studies has already been dedicated to porous nanostructured metal oxides, especially anatase TiO_2, many fundamental questions remain unanswered.[6] Some work has been done on single crystals to get a better understanding of the bulk properties of anatase TiO_2.[7-9] However, these crystals are reported to have a large number of defects and in some cases a high aluminium impurity content,[7] resulting in donor densities of the order of 10^{19} cm^{-3}, while porous nanostructured electrodes have donor densities of the order of 10^{17} cm^{-3}.[10,11] Since the donor density is expected to have a significant influence on various (opto-)electronic properties, the reported bulk properties for anatase single crystals may differ from those of porous nanostructured electrodes.

To overcome the complexities which are introduced by the porous topology while keeping the donor density comparable to that of porous films, very thin smooth films of TiO_2 are investigated here. These films possess a simple geometry while having a relatively high surface-to-volume ratio. They also have a comparable donor density, as will

be shown. Therefore, they offer interesting possibilities for studying (photoinduced) surface effects without some of the complicating factors found in porous films, *e.g.*, rate-determining electron transport phenomena through the porous structure. In this way thin smooth films of anatase TiO_2 can, to some degree of course, be regarded as a model system for their porous nanostructured counterparts.

This work shows that by using thin smooth films, the dielectric constant, the flatband potential, and the donor density of anatase TiO_2 can be accurately determined. The value found for the dielectric constant appears to be significantly lower than that commonly used in the literature for porous nanostructured anatase TiO_2.

Experimental

Thin anatase films were obtained by electron-beam evaporation of reduced rutile TiO_2 powder (Acros Chimica, 99.95+%) on tin-doped indium oxide (ITO) (80 nm ITO on glass, Glastron, 30 Ω/□) substrates. The substrate dimensions were typically 10 × 15 mm; the resistivity of the ITO was 2.4×10^{-6} Ω/cm. Reduction of TiO_2 was carried out in an atmosphere of hydrogen at 1000°C for 6 h. Deposition took place in a controlled 1×10^{-4} mbar O_2 atmosphere, with an argon background pressure smaller than 2×10^{-6} mbar. During deposition, the substrates were heated to 200°C. Additional depositions were made on nonheated substrates and without the oxygen partial pressure. Film growth was monitored with a quartz microbalance. Typical film thicknesses were 40 to 120 nm. After deposition, the samples were annealed at 450°C in air for 10 h in order to obtain the anatase structure. X-ray diffraction analysis was performed using a Philips PW1840 powder diffractometer using Cu k_α radiation.

Electrical contact to the TiO_2 films was made with a liquid junction in an electrochemical cell, since metallization led to short-circuiting via pinholes. The surface of the working electrode exposed to the electrolyte was circular, with a surface area of 7.0 mm^2. An electrochemical interface (Solartron Model 1286) and a frequency-response analyzer (Solartron Model 1250) were used to measure *I-V* characteristics, impedance spectra, and *C-V* curves. As electrolyte, a solution of 0.5 *M* KOH (pH 13.7) in demineralized and deionized water (ρ = 18.2 MΩ cm) was used. A saturated calomel electrode (SCE) served as reference electrode.

Results and Discussion

In Fig. 1 the film thickness is shown as a function of deposition time for a film grown to 80 nm. Films of 40 and 120 nm have been deposited under similar conditions. The growth process is linear in time, with typical deposition rates of 1.9 nm/min.

As-deposited films are amorphous, *i.e.*, x-ray Bragg reflections could not be observed. After annealing in air at 450°C, x-ray diffraction measurements, shown in Fig. 2, reveal that the films have a polycrystalline anatase structure. No traces of rutile are observed, which is in agreement with the fact that both deposition and annealing temperatures are well within the range where anatase formation is preferred. After annealing at 450°C for 1 h, crystallite sizes of 0.18 μm are obtained as derived from x-ray line broadening using Scherrer's equation.[12] After 10 h of annealing, the crystallite size increased to 0.31 μm. The x-ray diffraction peak of anatase powder (Janssen Chimica, 99%) at $2\theta = 25.39°$ is used as a reference value for the width at half height.

In both cases the apparent crystallite sizes are larger than the film thickness. Therefore, the shape of the crystallites cannot be spherical, which is assumed in Scherrer's equation. However, the volume of the particle, not the shape, is the dominant factor determining the amount of line broadening. Therefore, the crystallites are disk-shaped islands, with lateral dimensions of a few hundreds of nanometers.

I-V curves have been recorded for 40, 80, and 120 nm films in the potential range from 0 to −1.0 V *vs.* SCE. In Fig. 3 a voltammogram is shown for a film with a thickness of 80 nm, showing typical Schottky-barrier rectification. From −0.8 to −1.0 V *vs.* SCE the cathodic current density increases to a value of −67 μA cm^{-2}. Only the forward scan is shown in Fig. 3 since no hysteresis between the forward and the reverse scan is observed.

A typical Bode plot of the impedance measurements on an 80 nm thick film is shown in Fig. 4. The spectrum is recorded at a potential of −0.7 V *vs.* SCE, with a perturbation amplitude of 5 mV. The measured data have been fitted with a nonlinear least squares algorithm, from which a good fit is obtained when using the simple equivalent circuit shown in Fig. 4. In this equivalent circuit R is the combined resistance of the ITO and the electrolyte, and C represents a space-charge capacitance. The impedance of the constant-phase element, Q, can be written as $Z_Q = K(j\omega)^{-n}$, where K is a constant, ω is the angular frequency, and n describes the frequency behavior of the element. Q behaves as an ideal capacitance for $n = 1$, and an ideal

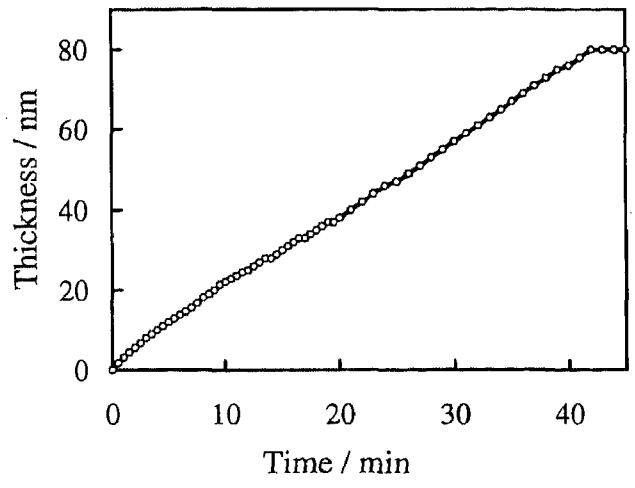

Fig. 1. Film thickness as a function of time during the electron-beam evaporation of reduced TiO_2 powder. A linear profile is observed with a growth rate of 1.9 nm/min. The substrate temperature is kept constant at 200°C during the deposition.

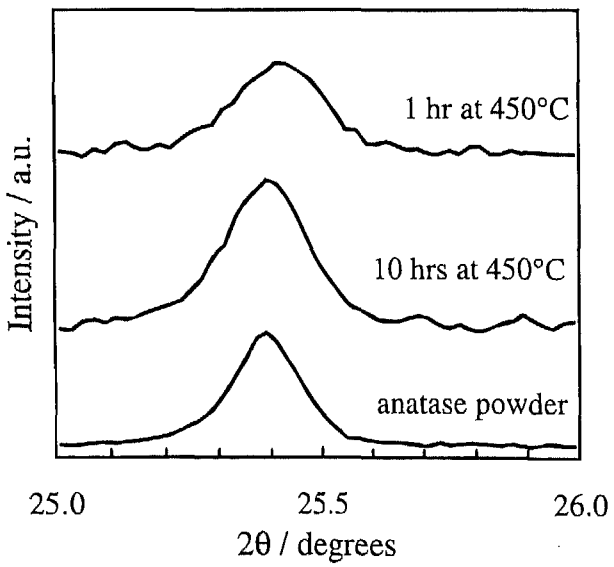

Fig. 2. X-ray diffraction peaks of 120 nm anatase TiO_2 films, annealed for both 1 h and 10 h at 450°C. Since the diffracted intensities are small for these thin films, only the highest intensity peak is shown. No x-ray diffraction peaks are observed before the annealing treatment.

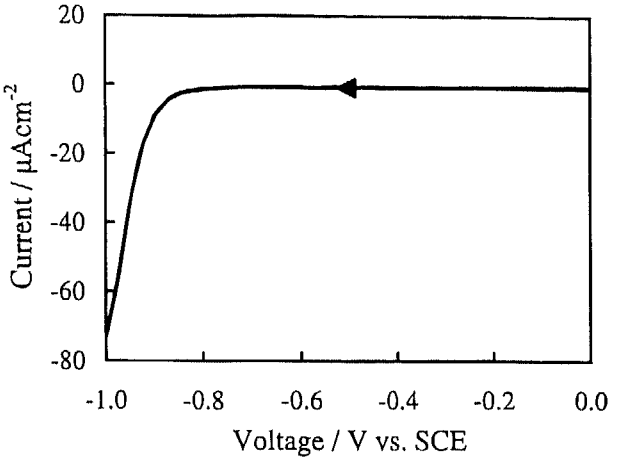

Fig. 3. Voltammogram of an 80 nm thick TiO_2 film on ITO, showing typical Schottky-barrier rectification. The voltammogram is recorded with a scan rate of 20 mV/s. Only the forward scan is shown, since no hysteresis between the forward and the reverse scan is observed.

resistance if $n = 0$. If $n = 0.5$ a Warburg element, which is often associated with semi-infinite diffusion, results. The following parameters are found from the fit of Fig. 4: R = 148 Ω, C = 10.5 nF, and $Q = 1.86 \times 10^{-8}$ Ω s^{-n}, with $n = 0.722$. The presence of the constant phase element is most likely caused by inhomogeneous transport phenomena, possibly in combination with a geometric capacitance. Its occurrence may also indicate interactions between current carrying defects. Another, unlikely possibility is that pinholes are involved. However, considering the film thicknesses of 80 and 120 nm, pinhole formation can be disregarded. A more detailed study of the origin of Q is beyond the scope of this work. At frequencies higher than 10 kHz the real part of the impedance reveals no frequency dependence, and the influence of Q on the impedance spectrum becomes negligible. In this part of the spectrum, the response of the system can be accurately described with an R-C series combination, with R and C having the values obtained from the fit results mentioned above.

Figure 5 presents typical Mott-Schottky plots of C^{-2} *vs.* V for 40, 80, and 120 nm thick films, recorded with a modulation frequency of 10 kHz and a scan rate of 1 mV/s. Almost identical curves are obtained when a modulation frequency of 50 kHz is used, which validates the capacitance measurements. Impedance measurements show that

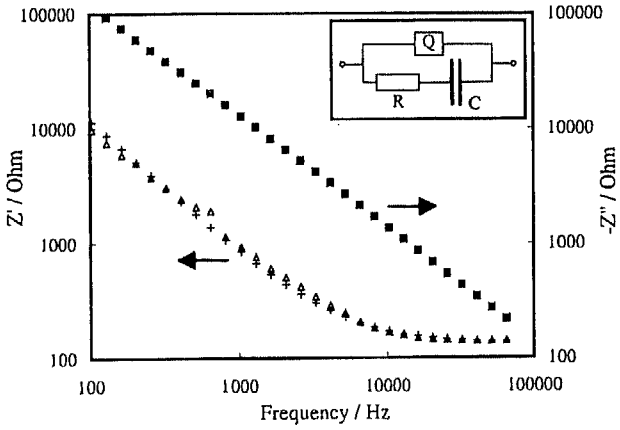

Fig. 4. Electrochemical impedance spectrum (Bode plot representation) of an 80 nm thick TiO_2 film on ITO, recorded at a potential of −0.7 V *vs.* SCE with a perturbation amplitude of 5 mV. The electrode surface area is 7.0 mm². (Δ) measured Z'; (+) simulated Z'; (□) measured Z''; (×) simulated Z''.

if frequencies of 10 kHz and higher are used, the equivalent circuit can be described by an R-C series combination. C can be easily derived from the imaginary part of the impedance, Z'', as a function of the applied bias potential, and Mott-Schottky plots can be constructed. The Mott-Schottky equation reads

$$\frac{1}{C^2} = \left(\frac{2}{e\epsilon_0\epsilon_r N_D A^2}\right)\left(\phi - \phi_{FB} - \frac{kT}{e}\right) \qquad [1]$$

where C is the differential capacitance of the space-charge region, ϵ_0 the permittivity of vacuum, ϵ_r the relative dielectric constant, N_D the donor density, A the surface area of the sample, ϕ the electrode potential, and ϕ_{FB} the flatband potential. In each curve in Fig. 5, two linear regions can be discerned, one between −1.0 and −0.8 V *vs.* SCE and the other at potentials positive of −0.7 V *vs.* SCE. The difference in the slopes of the two regions is discussed in the next paragraph. The flatband potentials for various film thicknesses (40, 80, and 120 nm) and at two different modulation frequencies (10 and 50 kHz) are determined by extrapolation of the linear region of the Mott-Schottky plot between −1.0 and −0.8 V *vs.* SCE, yielding a value of −0.98 ± 0.04 V *vs.* SCE. In all cases, the pH is fixed at 13.7. This value is in excellent agreement with reported values on thin smooth anatase films.[13,14]

Films deposited at a lower substrate temperature and with lower oxygen partial pressures are expected to have a larger defect concentration, in particular a larger concentration of oxygen ion vacancies. When Mott-Schottky plots of films with and without substrate heating are compared, the slope between −1.0 and −0.8 V *vs.* SCE for the films deposited without substrate heating is two orders of magnitude smaller, which corresponds to a two-orders-of-magnitude higher donor density (viz. Eq. 1). The other slope remains the same. Accordingly, the steep slope between −0.8 and −1.0 V *vs.* SCE can be attributed to the TiO_2 film, while the slope at $\phi > -0.7$ V *vs.* SCE is related to the ITO substrate. This interpretation of an abrupt change in slope for a Mott-Schottky plot is similar to that reported by Lincot *et al.*,[15] who used the same approach to monitor the growth of chemical-bath-deposited CdS. In order to describe the curved Mott-Schottky plot as observed in Fig. 5, an electrostatic model has been developed in which Schottky-barrier formation extending over two different semiconductor materials is considered (see

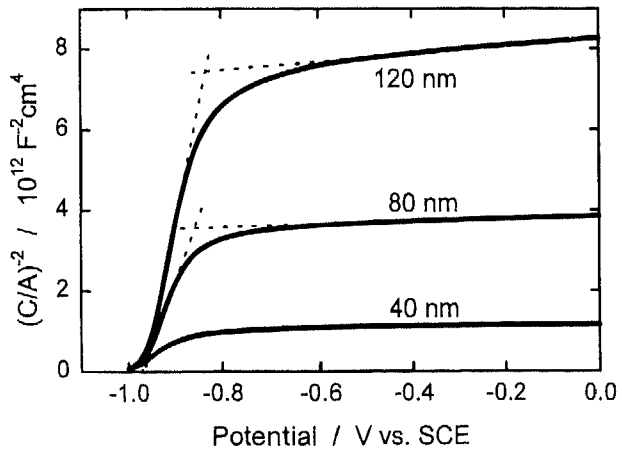

Fig. 5. Mott-Schottky plots of a 40, 80, and 120 nm thick TiO_2 film on ITO, recorded with a modulation frequency of 10 kHz, perturbation amplitude of 5 mV, and a scan rate of 1 mV/s. The capacitance plot is normalized to unit area using an electrode surface area of 7.0 mm² for all three films. At −0.8 V *vs.* SCE the depletion layer reaches the TiO_2/ITO interface, which is indicated by a change in slope. For clarity, only the forward scans are shown since the hysteresis between the forward and reverse scans is negligable.

Fig. 6). The mathematical analysis is given in the Appendix. It is shown that, if the depletion layer extends into the ITO layer, the slope of the curve is determined only by the dielectric constant and donor density of the ITO, and is not influenced by the TiO_2 film. From Fig. 5, the donor density of the ITO film is found to be $1 \times 10^{20} cm^{-3}$ when using a dielectric constant of 8.9, which is concordant with previously reported data for ITO films.[16] These results show that the change in slope observed from the Mott-Schottky plots represents the potential at which the depletion layer reaches the TiO_2/ITO interface.

The depletion-layer thickness, L_D, can be derived easily from Eq. 1 in combination with the parallel-plane capacitance approach, yielding

$$L_D = \left(\frac{2\epsilon_0\epsilon_r}{eN_D}\right)^{1/2}\left(\phi - \phi_{FB} - \frac{kT}{e}\right)^{1/2} \quad [2]$$

By eliminating the donor density from Eq. 1 and 2, the following expression for the depletion layer thickness is obtained

$$L_D = \epsilon_0\epsilon_r A S^{1/2}\left(\phi - \phi_{FB} - \frac{kT}{e}\right)^{1/2} \quad [3]$$

where S $(=2/\epsilon_0\epsilon_r eN_D A^2)$ is the slope of the Mott-Schottky curve. When the applied potential equals ϕ_i, the depletion layer has reached the TiO_2/ITO interface, and the value for L_D is equal to the TiO_2 film thickness. ϕ_i can be determined by extrapolating the two linear regions in the Mott-Schottky plot with $\phi = \phi_i$ at the point where the two lines cross; see Fig. 5. In this figure the dominant feature as a function of film thickness is the difference in magnitude of C^{-2} instead of the variation in potential drop across the film; the former is, of course, a consequence of the latter (and vice versa). Since the film thickness is known, the only adjustable variables are the surface area A and the dielectric constant ϵ_r. The exposed surface area is equal to the geometric surface area (*i.e.*, 7.0 mm^2), because electron-beam evaporation yields very smooth films. The dielectric constant can now be calculated. Following this procedure, values for ϵ_r of 48, 54, and 55 are found from Fig. 5 for anatase TiO_2 films of 40, 80, and 120 nm thickness, respectively. Analysis of Mott-Schottky plots recorded with 50 kHz yields similar values. The low value for the 40 nm films compared to the 80 and 120 nm films is not clear. Possibly it is the manifestation of a crystallite-size effect, since the dielectric constant is a macroscopic property. Although in thin-film studies pinhole formation can always compromise the results to some extent, this is not the case with our 80 and 120 nm films. For these films practically equal values for the dielectric constant are obtained. Since pinhole formation is known to have a significant influence on the capacitance (in our case a film with a 1% pinhole surface fraction will lead to a 10% lower capacitance), even small pinhole densities would be manifest in the calculated values for the dielectric constant. Obviously, this is not the case, which justifies our conclusion that for 80 and 120 nm TiO_2 films the influence of pinholes is insignificant. Based on these considerations, a value of 55 is proposed for the dielectric constant of polycrystalline anatase. This is in good agreement with the results found by Errera *et al.*,[17,18] who reported a value of 48 for anatase powder.

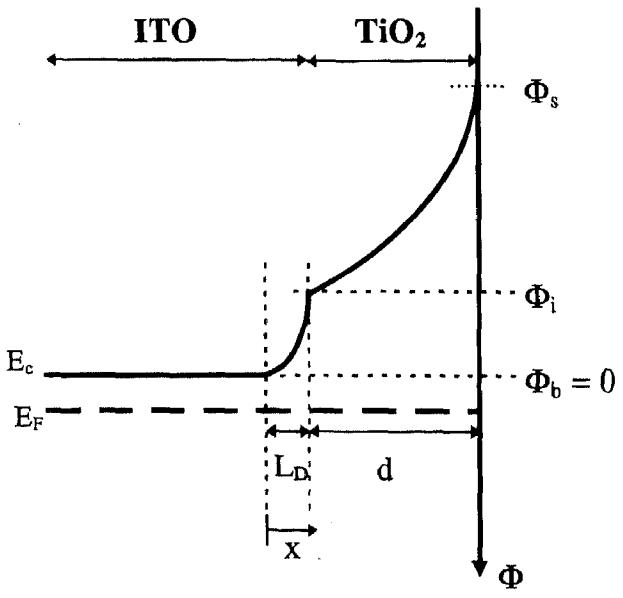

Fig. 6. Schematic energy diagram of a depleted two-layer semiconductor composite, where L_D is the length of the depleted region in the ITO; d, the TiO_2 film thickness; Φ_b, the potential in the bulk of the ITO; Φ_i, the potential at the interface; and Φ_s, the potential at the surface of the TiO_2.

The dielectric constant of rutile TiO_2, being 173 along the c-axis and 89 in the perpendicular direction,[18] is much larger than that of anatase. The difference in dielectric constants for anatase and rutile can be explained by considering the two crystal structures.[19] Both crystal structures are tetragonal with each Ti atom octahedrally coordinated to six O atoms, and each O atom coordinated to three Ti atoms. In both structures, the TiO_6 octahedra are slightly distorted, but the distortion is larger for anatase than that for rutile. In rutile, four Ti-O bonds of 1.949 Å and two Ti-O bonds of 1.980 Å are present. For anatase these values are 1.937 and 1.965 Å, respectively. Bond angles of O-Ti-O are 81.2° and 90.0° in rutile, whereas for anatase they are 77.7° and 92.6°, respectively. These values show that the TiO_6 octahedra in anatase are smaller than those in rutile. The polarizability of the titanium ions in anatase will therefore be smaller than that in rutile, which leads to a lower dielectric constant. Since the anatase structure is almost the same as the rutile structure, anisotropic behavior of the dielectric constant will be present. Therefore, the value of 55 for the dielectric constant of polycrystalline anatase is an average of the dielectric constants in the directions parallel and perpendicular to the c-axis.

Using the value for the dielectric constant of 55, the donor densities of the TiO_2 films can be calculated using Eq. 1. Values of 2.9×10^{17} cm^{-3} for 40 nm thick films, 7.9×10^{16} cm^{-3} for 80 nm thick films, and 4.1×10^{16} cm^{-3} for 120 nm thick films are found. Apparently, there is a systematic increase of the donor density when the film thickness is reduced. The nature of this remarkable effect is unclear and calls for further investigation.

Conclusions

Thin films of anatase TiO_2 have been successfully obtained by electron-beam evaporation of reduced TiO_2 powder. Mott-Schottky analysis clearly shows the potential at which the depletion layer reaches the TiO_2/ITO interface. From the position of this crossover point a dielectric constant of 55 is calculated for polycrystalline anatase. To date, most authors have used values ranging from 100 to 180 for the dielectric constant of porous nanostructured anatase films,[20-23] although values as low as 31 have also been assumed.[7,9] Present work on thin, smooth anatase films shows that the actual value is significantly lower than that of rutile TiO_2. Therefore, estimates of the dielectric constant of porous nanocrystalline anatase films based on values reported for rutile are in error. Also the values of the effective electron mass of nanocrystalline anatase based on the erroneous dielectric constant of 100 should be reconsidered. Since anatase has an anisotropic crystal structure, further research should be conducted on (high-purity) anatase single crystals to determine the dielectric constants in the directions parallel and perpendicular to the c-axis.

Errata

In the Appendix of the paper "Mott-Schottky Analysis of Nanometer-Scale Thin-Film Anatase TiO_2" by R. van de Krol, A. Goossens, and J. Schoonman that appeared on pp. 1723-1727 in the May 1997 Journal, Vol. 144, No. 5, the boundary condition for the electric field used in the derivation of the total capacitance of the system is in error. The correct boundary condition (boundary condition was unspecified in the original paper) for the electric field at the ITO/TiO_2 interface is $\epsilon_1 E(x{\downarrow}L_D) = \epsilon_2 E(x{\uparrow}L_D)$, which results in the following modified equations

$$E(x \geq L_D) = (N_{D2} - N_{D1})\frac{eL_D}{\epsilon_1} + \left(\frac{eN_{D1}}{\epsilon_1}\right)x \qquad \text{[A-5]}$$

$$\Phi(x \geq L_D) = \left(\frac{eN_{D2}}{\epsilon_1} - \frac{eN_{D2}}{2\epsilon_2} - \frac{eN_{D1}}{2\epsilon_1}\right)L_D^2 + \left(\frac{e(N_{D1} - N_{D2})}{\epsilon_1}\right)L_D x - \left(\frac{eN_{D1}}{2\epsilon_1}\right)x^2 \qquad \text{[A-8]}$$

$$\Phi_{SC} = -\Phi_S = \left(\frac{eN_{D2}}{2\epsilon_2}\right)L_D^2 + \left(\frac{eN_{D2}d}{\epsilon_1}\right)L_D + \left(\frac{eN_{D1}d^2}{2\epsilon_1}\right) \qquad \text{[A-9]}$$

$$L_D = -\frac{\epsilon_2 d}{\epsilon_1} \pm \left\{\left(1 - \frac{\epsilon_1 N_{D1}}{\epsilon_2 N_{D2}}\right)\left(\frac{\epsilon_2 d}{\epsilon_1}\right)^2 + \left(\frac{2\epsilon_2}{eN_{D2}}\right)\Phi_{SC}\right\}^{1/2} \qquad \text{[A-10]}$$

$$Q_S = \left(N_{D1} - \frac{\epsilon_2}{\epsilon_1}N_{D2}\right)ed + \left\{\left(1 - \frac{\epsilon_1 N_{D1}}{\epsilon_2 N_{D2}}\right)\left(\frac{e\epsilon_2 N_{D2}d}{\epsilon_1}\right)^2 + 2\epsilon_2 eN_{D2}\Phi_{SC}\right\}^{1/2} \qquad \text{[A-11]}$$

$$C = \frac{dQ_S}{d\Phi_{SC}} = (\epsilon_2 eN_{D2})\left\{\left(1 - \frac{\epsilon_1 N_{D1}}{\epsilon_2 N_{D2}}\right)\left(\frac{e\epsilon_2 N_{D2}d}{\epsilon_1}\right)^2 + 2\epsilon_2 eN_{D2}\Phi_{SC}\right\}^{-1/2} \qquad \text{[A-13]}$$

$$\frac{1}{C^2} = \left(1 - \frac{\epsilon_1 N_{D1}}{\epsilon_2 N_{D2}}\right)\left(\frac{d}{\epsilon_1}\right)^2 + \left(\frac{2}{\epsilon_2 eN_{D2}}\right)\Phi_{SC} \qquad \text{[A-14]}$$

The modifications in Eq. A-14 concern only the offset of the $C^{-2} - \Phi_{SC}$ curve. The slope of the curve, from which the donor density in the ITO is calculated, has not changed. Therefore, these corrections do not change the main conclusion of the model, i.e., the slope of the Mott-Schottky curve when the depletion layer has entered the second layer (ITO) is solely determined by the dielectric constant the donor density of this layer.